Proceedings of the 38th Chinese Control Conference
July 27-30, 2019, Guangzhou, China

Distributed Connectivity Maintenance and Collision Avoidance Control of Spacecraft Formation Flying

Xianghong Xue[1], Xiaokui Yue[1], JianPing Yuan[1]
1. National Key Laboratory of Aerospace Flight Dynamics, Northwestern Polytechnical University, Xi'an 710072, P. R. China
E-mail: xhxue@mail.nwpu.edu.cn

Abstract: This paper studies the distributed control of spacecraft formation flying with collision avoidance and connectivity maintenance. Until now, almost all studies do not consider the impact of the spacecraft's relative position on the communication graph between spacecraft, instead, merely assume that the communication graph satisfies certain connectivity conditions, such as connectivity of an undirected graph, strong connectivity of a directed graph, or joint connectivity of a switching graph. This paper proposes a distributed connectivity maintenance controller to ensure the connectivity of communication graph during spacecraft formation flying. First, a dynamic graph based on the relative distance between the spacecraft is employed to model the real-time communication graph. In addition, two artificial potential functions, respectively, regarded as the repulsive force and the attractive force, are established to preserve the graph connectivity and avoid the collisions at the same time. A distributed connectivity preserving control law is proposed to eliminate the computing burden of a single satellite and enhance the reliability of the spacecraft system. The distributed control algorithm ensures that if the graph is connected at the initial time, then it will connect in the future. The mass uncertainties are also taken into account for implementation in the complex space environment. Numerical simulations of the proposed method are presented to show the effectiveness of the distributed controller during spacecraft formation flying.

Key Words: Spacecraft formation flying, Connectivity maintenance, Collision avoidance,Distributed control

1 Introduction

Spacecraft formation flying (SFF) is defined as the tracking or maintenance of a desired relative separation, orientation or position between or among spacecraft [1]. It has aroused much interests owing to its the obvious advantages compared with a single traditional monolithic spacecraft, such as flexibility, reliability, robustness and low fuel consumption [2]. These advantages make SFF being a competitive method to implement synthetic aperture radars, gravity field measurement, space-based interferometers and distributed satellite architecture. [3–5].

Compared with the monolithic spacecraft, all spacecraft in formation needs to communicate with each other. Therefore, one challenge related to SFF is how to design a distributed coordination controller for SFF [6]. According to the task requirements, formation control methods specify the task into different behaviors, such as collision avoidance, formation tracking, formation maintenance and formation reconfiguration [7, 8]. In practical applications, collision avoidance is the fundamental requirements for formation flying and the prerequisite for all the other tasks previously mentioned such as formation maintaining and reconstruction. In literature [2], the authors presented a behavioral control solution using the Null-Space Based (NSB) concept for spacecraft formation reconfiguration and collision avoidance. Zhou et al. proposed a finite-time coordination control scheme with NSB concept for SFF to avoid the collision [9]. In this work, the controller can accomplish the formation reconfiguration task in unknown obstacle environments without using an accurate mathematical model. Hu et al. studied nonlinear adaptive feedback control of SFF with avoiding obstacles and maintaining the formation configuration [10]. Ref. [11] presented a tracking control scheme of a virtual leader for spacecraft formation flying with a decentralized collision avoidance scheme. The configuration space for a spacecraft is the Lie group SE(3), which is the set of positions and orientations in three-dimensional Euclidean space. Unlike the model used in [11], Ref. [12] investigates the collision-free distributed coordination control of six-DOF SFF by dual quaternions.

Another challenge in SFF is how to model and construct the communication graph in SFF, as it is time-varying and impacted by the relative distance between spacecraft. However, almost all studies assume that the communication graphs are connected during formation maintenance and formation reconfiguration. Practically, these assumptions are hard to meet. Connectivity maintenance for single and second order system had been studied in [13, 14]. However, these results can not directly be applied to nonlinear spacecraft dynamics. The main purpose of this paper is to propose a distributed coordination control for SFF with collision avoidance and connectivity maintenance. Firstly, suppose the sensing region of the spacecraft is a sphere and then the communication graph is constructed dynamically according to the relative distance between spacecraft. The collision region is also modeled as a sphere and involved in the construction of the graph. In addition, two artificial potential functions, including attraction function and repulsion function, are presented to provide the attractive force and repulsive force. Moreover, a control law based on artificial function and certainty equivalence principle are designed. Finally, LaSalle's invariance principle was employed to ensure the algorithm can not only preserve the connectivity of the graph and avoid the collisions between all spacecraft.

The paper is organized as follows: Section 2 states the relative dynamics of spacecraft formation system and some notions about algebra graph theory. The potential functions and control method is proposed in Section 3. Numerical simulations are presented in Section 4 to demonstrate various features and effectiveness of the proposed control methods. Finally, the paper is completed with some concluding comments in Section 5.

2 Problem statement

In this paper, we mainly study how to maintain connectivity of the communication graph and avoid collisions between all spacecraft during formation reconfiguration. This section provides the relative dynamics of spacecraft and some notions of algebra graph theory.

2.1 Spacecraft dynamics

It is assumed that all spacecraft are rigid and the reference spacecraft transits in an elliptical orbit. The reference frame, denoted by $\mathcal{F}^r$, has its origin at the centroid of the reference spacecraft. The X_r axis points from the earth center to the reference spacecraft, the Z_r axis is perpendicular to the reference orbit plane, and the Y_r axis can be obtained according to the right-hand rule. Noting that throughout this paper, except special explanation, every three-dimensional column vector can be written as the decomposition form $\boldsymbol{l}_{3\times1} = [l_x, l_y, l_z]^T$ to represent the component of each axis with respect to the reference orbital coordinate system. Consider a system with N spacecraft, ρ_i and v_i denote the position and the velocity of the i-th spacecraft in the formation with respect to the reference orbit frame, respectively. Then, the relative dynamics can be described by [15]

$$\begin{aligned}\dot{\boldsymbol{\rho}}_i =& \boldsymbol{v}_i \\ m_i\dot{\boldsymbol{v}}_i =& \boldsymbol{C}_i(\dot{\theta}_c)\boldsymbol{v}_i + \boldsymbol{D}_i(\ddot{\theta}_c, \dot{\theta}_c, ||\boldsymbol{r}_i||)\rho_i + \boldsymbol{n}_i(||\boldsymbol{r}_i||, ||\boldsymbol{r}_c||) + \boldsymbol{f}_i\end{aligned} \tag{1}$$

where

$$\boldsymbol{C}_i(\dot{\theta}_c) = 2m_i\dot{\theta}_c \begin{bmatrix} 0 & 1 & 0 \\ -1 & 0 & 0 \\ 0 & 0 & 0 \end{bmatrix} \tag{2}$$

$$D_i(\ddot{\theta}_c, \dot{\theta}_c, \boldsymbol{r}_i) = -m_i\frac{\mu}{r_i^3}\boldsymbol{I}_{3\times3} + m_i \begin{bmatrix} \dot{\theta}_c^2 & \ddot{\theta}_c & 0 \\ -\ddot{\theta}_c & \dot{\theta}_c^2 & 0 \\ 0 & 0 & 0 \end{bmatrix} \tag{3}$$

$$\boldsymbol{n}_i(||\boldsymbol{r}_i||, ||\boldsymbol{r}_c||) = \mu m_i \left[-\frac{||\boldsymbol{r}_c||}{||\boldsymbol{r}_i||^3} + \frac{1}{||\boldsymbol{r}_c||^2},\ 0,\ 0\right]^T \tag{4}$$

and m_i is the mass of the i-th spacecraft, θ_c is the true anomaly of the reference spacecraft, $||\boldsymbol{r}_c||$ ($||\cdot||$ presents the Euclidean norm of a vector throughout this paper) denotes the distance between the centroid of the reference spacecraft and the Earths center, μ is the gravitational constant of the Earth, $\boldsymbol{f}_i$ is the control force vector of the i-th spacecraft, $||\boldsymbol{r}_i|| = \sqrt{(||\boldsymbol{r}_c|| + \rho_{ix})^2 + \rho_{iy}^2 + \rho_{iz}^2}$ is the distance between the centroid of the i-th spacecraft and the Earths center.

Assumption 1. *Since the mass change of the spacecraft in formation is very small, the mass m_i is assumed constant but unknown.*

2.2 Algebraic graph theory

During formation flying, each spacecraft receives the states of other spacecraft through communication graph (through data transmission and measurement equipment) to achieve formation task. The communication graph between all spacecraft is described by graph theory in this paper. This subsection presents some notions of algebraic graph theory [16]. A weighted graph $\mathcal{G}$ is an ordered triple $(\mathcal{V}, \mathcal{E}, A(\mathcal{G}))$ consisting a vertex set $\mathcal{V} = \{1, 2, \dots N\}$, an edge set $\mathcal{E} \subset \mathcal{V} \times \mathcal{V}$ and a weighted adjacency matrix $\boldsymbol{A} = [a_{ij}] \in \mathbb{R}^{n\times n}$. The edge $(i, j) \in \mathcal{E}$ if and only if the vertex j can get information from vertex i. In this situation, the i-th and j-th spacecraft are called adjacent. Graph $\mathcal{G}$ is said to be undirected if for any edge $(i, j) \in \mathcal{E}$, $(j, i) \in \mathcal{E}$. The set of neighbors of the i-th spacecraft is denoted by $\mathcal{N}_i = \{j \in \mathcal{V}, (i, j) \in \mathcal{E}\}$. A path of length m in $\mathcal{G}$ is given by a sequence of distinct vertices $v_{i_0}, v_{i_1}, \dots, v_{i_m}$ such that for $k = 0, 1, \dots, m-1$, the vertices v_{i_k} and $v_{i_{k+1}}$ are adjacent. The graph $\mathcal{G}$ is called a connected graph if there is a path for every pair of vertices in $\mathcal{V}$. The adjacency matrix $A(\mathcal{G})$ of $\mathcal{G}$ is defined such that $a_{ij} = a_{ji}$ is a positive weight if $(i, j) \in E(\mathcal{G})$, otherwise $a_{ij} = 0$. Another important matrix of graph $\mathcal{G}$ is the Laplacian matrix $\boldsymbol{L} = [l_{ij}] \in \mathbb{R}^{n\times n}$, which is defined as: if $i = j$, $l_{ij} = \sum_{j=1}^{N} a_{ij}$, otherwise $l_{ij} = -a_{ij}$.

Lemma 1. *The Laplacian matrix L is symmetric and positive semidefinite [16].*

2.3 Control objective

By utilizing the artificial function, we aim to design a distributed control law for each spacecraft to reconfigure all spacecraft to the desired relative position even the mass of spacecraft is unknown. Meanwhile, the proposed methods can maintain the connectivity of communication graph and avoid the collisions between all spacecraft at the same time.

Connectivity maintenance means keeping the communication graph of the spacecraft system connected at any time. Collision avoidance is defined as avoiding collisions between spacecraft. Figure 1 shows the sectional drawing of the sensing sphere region with radius Δ and the collision sphere region with radius δ of spacecraft i. Spacecraft j is on the boundary of collision region and spacecraft l is out of the sensing region of spacecraft i. These two spacecraft have no communication with spacecraft i. Spacecraft k is in the sensing region and out the collision region of spacecraft i, therefore, they can communicate with each other. The purpose of connectivity maintenance control is to preserve spacecraft like k being in the sensing region of spacecraft i. The collision avoidance control is to avoid the distance between any two spacecraft smaller than δ.

3 Main results

3.1 Dynamic graph construction

The dynamic graph $\mathcal{G}(t) = (\mathcal{V}, \mathcal{E}(t))$ is generated according to the positions of all spacecraft. Let $\epsilon \in (\Delta - \delta, \Delta)$ be a given constant. The time-varying edge set is defined as

(i) initial edges are generated by $\mathcal{E}(0) = \{(i, j)|\ ||\boldsymbol{\rho}_{ij}|| \in (\delta + \epsilon, \Delta - \epsilon), i, j \in \mathcal{V}\}$.

(ii) if $(i, j) \notin \mathcal{E}(t^-)$ and $||\boldsymbol{\rho}_{ij}|| \in (\delta + \epsilon, \Delta - \epsilon)$, then (i, j) is added to $\mathcal{E}(t)$.

(iii) if $(i, j) \in \mathcal{E}(t^-)$ and $||\boldsymbol{\rho}_{ij}|| > \Delta - \epsilon$, then (i, j) is deleted from $\mathcal{E}(t)$.

(iv) if $(i, j) \in \mathcal{E}(t^-)$ and $||\boldsymbol{\rho}_{ij}|| < \delta + \epsilon$, then (i, j) is deleted from $\mathcal{E}(t)$.

Remark 1. From the upper process, we know that the pur-

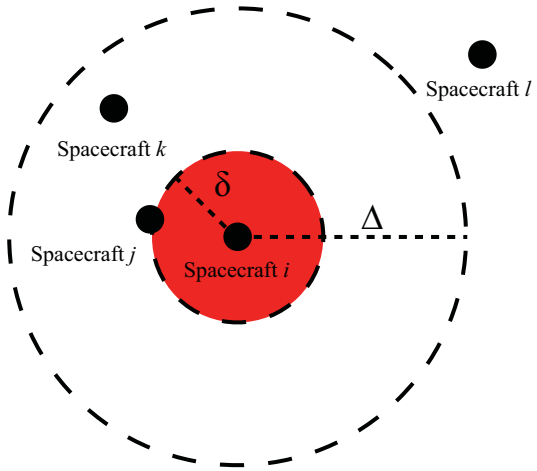

Fig. 1: Sectional drawing of the sense and collision region

pose of step (ii) is to add an edge to the dynamic graph and step (iii) and step (iv) are to delete an edge. In fact, the latter two steps will not occur under the distributed connectivity maintenance control laws proposed in this paper.

The former procedure can be represented by a time-varying indicator matrix $\sigma_{ij}(t) \in \{0, 1\}$, which is defined as

$$\sigma_{ij}(0) = \begin{cases} 1, & \text{if } ||\boldsymbol{\rho}_{ij}(0)|| \in (\delta + \epsilon, \Delta - \epsilon), i, j \in \mathcal{V}\} \\ 0, & \text{otherwise.} \end{cases} \tag{5}$$

$$\sigma_{ij}(t) = \begin{cases} 1, & \text{if } (\sigma_{ij}(t^-) = 1) \cap (||\boldsymbol{\rho}_{ij}(t)|| \in (\delta, \Delta)) \\ & \quad \cup (\sigma_{ij}(t^-) = 0) \cap (||\boldsymbol{\rho}_{ij}(t)|| \in [\delta + \epsilon, \Delta - \epsilon]) \\ 0, & \text{otherwise.} \end{cases} \tag{6}$$

With the indicator matrix, the elements of the dynamic adjacency matrix $A(t)$ of dynamic graph $\mathcal{G}(t)$ is given as

$$a_{ij}(t) = \sigma_{ij}(t) \cdot w_{ij} \tag{7}$$

Assumption 2. *It is assumed that each spacecraft has the same sensing radius Δ to ensure the communication edge, and the same minimum distance δ to avoid collisions.*

Assumption 3. *The desire distance of formation flying satisfies*

$$d_{ij} \in (\delta, \Delta), \text{ and } d_{ij} = d_{ji}, \text{for all } (i, j) \in \mathcal{E}. \tag{8}$$

The minimum distance δ in Assumption 2 can be different for each spacecraft, and this condition does not effect the results in this paper. However, the sensing radius Δ needs to be equal for all spacecraft. Equal sensing radius implies the communication graph is an undirected graph.

Assumption 4. *Suppose no collision has happened before the initial time, which implies the distance between all spacecraft are greater than $\delta + \epsilon$, i.e. $||\boldsymbol{\rho}_{ij}|| > \delta + \epsilon, \forall\, i, j = 1, \ldots, N$.*

3.2 Artificial potential function

Artificial potential function $J(||\boldsymbol{\rho}_{ij}||)$ is a function of the distance $||\boldsymbol{\rho}_{ij}||$ between spacecraft i and j. The potential function consists of two parts, one is the attraction function $J_a(||\boldsymbol{\rho}_{ij}||)$ to preserve connectivity and the other is the repulsion function $J_r(||\boldsymbol{\rho}_{ij}||)$ to avoid collision. In particular, $J(||\boldsymbol{\rho}_{ij}||)$ is defined as

$$\begin{aligned} J(||\boldsymbol{\rho}_{ij}||) =& J_a(||\boldsymbol{\rho}_{ij}||) + J_r(||\boldsymbol{\rho}_{ij}||) \\ =& J^a_{ij} + J^r_{ij} \end{aligned} \tag{9}$$

There are some requirements and assumptions for each part of potentials:

(i) $J(||\boldsymbol{\rho}_{ij}||)$ is differentiable with respect to $||\boldsymbol{\rho}_{ij}|| \in [\delta, \Delta]$.

(ii) $J(||\boldsymbol{\rho}_{ij}||)$ is symmetric and satisfies

$$\nabla_{\rho_i} J(||\boldsymbol{\rho}_{ij}||) = -\nabla_{\rho_j} J(||\boldsymbol{\rho}_{ij}||) \tag{10}$$

where $\nabla_{\rho_i} J_{ij}$ denotes the gradient of J_{ij} with respect to ρ_i.

(iii) Artificial function $J(||\boldsymbol{\rho}_{ij}||)$ attains its unique minimum when $(||\boldsymbol{\rho}_{ij}||)$ equals the desired distance d_{ij}, that is

$$\nabla_{\rho_i} J(||\boldsymbol{\rho}_{ij}||) = 0, \text{if and only if } ||\boldsymbol{\rho}_{ij}|| = d_{ij}. \tag{11}$$

(iv) Attraction function $J_a(||\boldsymbol{\rho}_{ij}||)$ is a monotonically increasing function with respect to $||\boldsymbol{\rho}_{ij}||$, and $J_a(||\boldsymbol{\rho}_{ij}||) \to \infty$ as $||\boldsymbol{\rho}_{ij}|| \to \Delta$.

(v) Repulsion function $J_r(||\boldsymbol{\rho}_{ij}||)$ is a monotonically decreasing function with respect to $||\boldsymbol{\rho}_{ij}||$, and $J_r(||\boldsymbol{\rho}_{ij}||) \to \infty$ as $||\boldsymbol{\rho}_{ij}|| \to \delta$.

(vi) $J(||\boldsymbol{\rho}_{ij}||) \to \infty$ as $||\boldsymbol{\rho}_{ij}|| \to \Delta$ and $||\boldsymbol{\rho}_{ij}|| \to \delta$.

An example of attraction function and repulsion function is given as

$$\begin{aligned} J^a_{ij} = J^a(||\boldsymbol{\rho}_{ij}||) &= \begin{cases} \frac{(||\boldsymbol{\rho}_{ij}||^2 - ||d_{ij}||^2)^2}{(\Delta^2 - ||\boldsymbol{\rho}_{ij}||^2)^2}, & \text{if } (i, j) \in E(t) \\ 0, & \text{otherwise.} \end{cases} \\ J^r_{ij} = J^r(||\boldsymbol{\rho}_{ij}||) &= \begin{cases} \frac{(||\boldsymbol{\rho}_{ij}||^2 - ||d_{ij}||^2)^2}{(||\boldsymbol{\rho}_{ij}||^2 - \delta^2)^2}, & \text{if } (i, j) \in E(t) \\ 0, & \text{otherwise.} \end{cases} \end{aligned} \tag{12}$$

Remark 2. The repulsion function provides a repulsive force for any two spacecraft if their distance is in $(\delta, d_{ij}]$. On the other hand, the attraction function provides an attractive force for two spacecraft if their distance is in $[d_{ij}, \Delta)$.

3.3 The control scheme

The control input in Eq. (1) is specified as

$$\begin{aligned} \boldsymbol{f}_i =& K_f \sum_{j=1}^{N} a_{ij}(t)(\boldsymbol{v}_j - \boldsymbol{v}_i) - K_p \sum_{\substack{j \neq i \\ j=1}}^{N} a_{ij}(t) \nabla_{\boldsymbol{\rho}_i} J_{ij} + \hat{m}_i \boldsymbol{F}_i \\ \dot{\hat{m}}_i =& -\alpha \boldsymbol{v}_i^T \boldsymbol{F}_i \end{aligned} \tag{13}$$

where $\hat{m}_i$ is the estimation of m_i, $\tilde{m}_i = m_i - \hat{m}_i$, α is a positive constant, and $\boldsymbol{F}_i$ is defined as

$$\boldsymbol{F}_i = -\frac{1}{m_i}(\boldsymbol{D}_i \boldsymbol{\rho}_i + \boldsymbol{n}_i), \tag{14}$$

which is independent of m_i.

Theorem 1. *Consider a system of N spacecraft with dynamics Eq. (1) and Assumption 1-4, each steered by protocol Eq. (13). Assume that the initial graph $\mathcal{G}(0)$ is connected. Then, the following hold:*

(i) $\mathcal{G}(t)$ is connected for all $t > 0$.
(ii) There are no collisions between any two spacecraft.
(iii) $||\boldsymbol{\rho}_{ij}|| \to d_{ij}$ as $t \to \infty$ for all $(i,j) \in \mathcal{E}$.
(iv) All spacecraft asymptotically converge to equal velocity.

Proof. Suppose that $\mathcal{G}(t)$ switches at time $t_k (k = 1, 2, \ldots)$, otherwise $\mathcal{G}(t)$ is a fixed graph in each time interval $[t_{k-1}, t_k]$. Define a Lyapunov function

$$V(t) = \frac{1}{2}\sum_{i=1}^{N} m_i \boldsymbol{v}_i^T \boldsymbol{v}_i + \frac{K_p}{2}\sum_{i=1}^{N}\sum_{j\neq i}^{N} a_{ij} J_{ij} + \frac{1}{2\alpha}\sum_{i=1}^{N} \tilde{m}_i^2 \tag{15}$$

Since $\mathcal{G}(0)$ is connected and no collisions have happened at time t_0, the definition of $V(t)$ implies that $V(t)$ is finite at $t = 0$.

Taking the derivative of Eq. (15) in $[t_0, t_1]$ and substituting Eq. (1), (13) and (14) yields

$$\begin{aligned}
\dot{V}(t) =& \sum_{i=1}^{N} m_i \boldsymbol{v}_i^T \dot{\boldsymbol{v}}_i + \frac{K_p}{2}\sum_{i=1}^{N}\sum_{j\neq i}^{N} a_{ij}(t)\dot{J}_{ij} - \sum_{i=1}^{N}\frac{1}{\alpha}\tilde{m}_i\dot{\hat{m}}_i \\
=& \sum_{i=1}^{N} \boldsymbol{v}_i^T \Bigg[\boldsymbol{C}_i \boldsymbol{v}_i + \boldsymbol{D}_i \boldsymbol{\rho}_i + \boldsymbol{n}_i + K_f \sum_{j\neq i}^{N} a_{ij}(t)(\boldsymbol{v}_j - \boldsymbol{v}_i) \\
& - K_p \sum_{j\neq i}^{N} a_{ij}(t) \nabla_{\boldsymbol{\rho}_i} J_{ij} + \hat{m}_i \boldsymbol{F}_i \Bigg] + \sum_{i=1}^{N} \tilde{m}_i \boldsymbol{v}_i^T \boldsymbol{F}_i \\
& + \frac{K_p}{2}\sum_{i=1}^{N}\sum_{j\neq i}^{N} a_{ij}(t) \left[\nabla_{\boldsymbol{\rho}_i}^T J_{ij} \dot{\boldsymbol{\rho}}_i + \nabla_{\boldsymbol{\rho}_j}^T J_{ij} \dot{\boldsymbol{\rho}}_j \right] \\
=& K_f \sum_{i=1}^{N}\sum_{j\neq i}^{N} a_{ij}(t) \boldsymbol{v}_i^T (\boldsymbol{v}_j - \boldsymbol{v}_i) \\
=& K_f \sum_{i=1}^{N}\sum_{j\neq i}^{N} a_{ij}(t) (-\boldsymbol{v}_i^T \boldsymbol{v}_i + \boldsymbol{v}_i^T \boldsymbol{v}_j) \\
=& -K_f \boldsymbol{v}^T \left[\boldsymbol{L}(t) \otimes \boldsymbol{I}_N \right] \boldsymbol{v}
\end{aligned} \tag{16}$$

where $\boldsymbol{v} = [\boldsymbol{v}_1^T, \boldsymbol{v}_2^T, \ldots, \boldsymbol{v}_N^T]^T$ denotes the vector consist by all spacecraft's velocity. The equation $\sum_{i=1}^{N} \boldsymbol{v}_i^T \boldsymbol{C} \boldsymbol{v}_i = 0$ is used in Eq. (16).

According to Lemma 1, $\boldsymbol{L}(t)$ is positive semi-definite, and then $\dot{V}(t) \leq 0$ in $[t_0, t_1]$. It dictates that $V(t) \leq V(0)$ for $t \in [t_0, t_1]$. Without loss of generality, assume that m_1 new links are added to the dynamic communication graph at time t_1. Clearly, $0 < m_1 < M$ and $M = \frac{(N-1)(N-2)}{2}$, thus $V(t_1) < V_0 + m_1(J(||\Delta - \epsilon||) + J(||\delta + \epsilon||) < V_{\max}$, where $V_{\max} = \frac{1}{2}\sum_{i=1}^{N} m_i v_i(0)^T v_i(0) + \frac{N(N-1)}{2}(J(||\Delta - \epsilon||) + J(||\delta + \epsilon||) + \sum_{i=1}^{N} \frac{1}{2\alpha}\tilde{m}_i(0)^2$. Similar to the aforementioned analysis, the time derivative of $V(t)$ in $[t_{k-1}, t_k]$ is

$$\dot{V}(t) = -\boldsymbol{v}^T \left[\boldsymbol{L}(t) \otimes \boldsymbol{I}_N \right] \boldsymbol{v} \leq 0 \tag{17}$$

which implies that

$$V(t) \leq V(t_{k-1}) < V_{\max} \text{ for } t \in [t_{k-1}, t_k], k = 1, 2, \ldots. \tag{18}$$

From the definition of the potential function, one has $J(t) < V(t) < J(\Delta)$ and $J(t) < V(t) < J(\delta)$. This guarantee that $J(t)$ is finite for all $t > 0$ and this implies no edge-distance will tend to Δ and δ for $t > 0$. Therefore, no existing edges will be lost and no collisions will happen between any two spacecraft. Since $\mathcal{G}(0)$ is connected and no edges in $\mathcal{E}(0)$ will be lost, $\mathcal{G}(t)$ will be connected for all $t \geq 0$.

From $V(t) \leq V_{\max}$, one can get $\boldsymbol{v}_i^T \boldsymbol{v}_i \leq \frac{2V_{\max}}{m_i}$ and $\boldsymbol{v}_i$ is bounded. Thus, $\dot{V}$ is bounded and then $\ddot{V}$ is bounded too. Using Barbalat's lemma one has $\lim_{t\to\infty} \dot{V} = 0$. From (16), we known that $\dot{V} = 0$ if and only if $\boldsymbol{v}_1 = \boldsymbol{v}_2 = \cdots = \boldsymbol{v}_N$, which implies that all spacecraft asymptotically converge to the same velocity.

The property (iii) of artificial function implies that $J(||\boldsymbol{\rho}_{ij}||)$ attains its unique minimum when $(||\boldsymbol{\rho}_{ij}||)$ equals the desired distance d_{ij}. Thus, if edge $(i,j) \in \mathcal{E}$, $||\boldsymbol{\rho}_{ij}|| \to d_{ij}$ as $t \to \infty$. With Assumption 3, one can get that $||\boldsymbol{\rho}_{ij}|| \to d_{ij}$ as $t \to \infty$ for all $(i,j) \in \mathcal{E}$. ■

Remark 3. It is important to note that the addition of ϵ in Eq. (6) is to avoid artificial function J to be infinite. More precisely, it ensures the control input will be finite.

Remark 4. In literature [13], the control law ensures the distance between any two agents is only possible to decrease. However, this property can not been provided in this paper as the potential function contains the repulsion function as well as the attraction function.

4 Simulations

To demonstrate the effectiveness of the proposed control in Eqs. (13), the detailed responses are numerically simulated using the set of governing equation Eqs. (1) in conjunction with the potential function in Eqs. (12).

For the numerical examples given in this section, the parameters of reference orbit are provided in Table 1. It is assumed that all components of a spacecraft can be wrapped by a sphere with radius is $5m$. In this case, one can easily choose $\delta = 10m$ to satisfy the anti-collision requirement. In addition, supposing the sensing radius of all spacecraft is $\Delta = 120m$, the masses of each spacecraft are $m_1 = 100kg$, $m_2 = 120kg$, and $m_3 = 115kg$, and the initial masses estimation are set to $\hat{m}_1 = \hat{m}_2 = \hat{m}_3 = 110kg$.

Table 1: Parameters for the reference orbit

Orbital parameters	Value
Eccentricity	0.02
Inclination	30°
Longitude ascending node	45°
Semi-major axis	$7000km$
Argument of perigee	30°
Initial true anomaly	0°
Gravitational constant	$3.986 \times 10^{14}(m^3/s^2)$

The control and initialization parameters are given in Table 2. From the table, one can compute the distance between all spacecraft at the initial time: $||\boldsymbol{\rho}_{12}|| = 25.45m$,

$||\boldsymbol{\rho}_{13}|| = 84.9m$, $||\boldsymbol{\rho}_{12}|| = 60m$. Therefore, the initial graph is a complete graph.

Table 2: Symbols used in simulations

Parameters	Value
$\boldsymbol{\rho}_1(0)$	$[0, 30, 0]^T\ m$
$\boldsymbol{\rho}_2(0)$	$[0, 12, 0]^T\ m$
$\boldsymbol{\rho}_3(0)$	$[0, -30, 30]^T\ m$
$\boldsymbol{v}_i(0)$	$[0, 0, 0]^T\ (m/s)$, for $i = 1, 2, 3$
d_{ij}	$60m$, for $i, j = 1, 2, 3$
w_{ij}	1, for $i, j = 1, 2, 3$
K_f	0.3
K_p	0.3
α	5

Figs. 2, 3 and 4 show the results of velocity errors, distance and control force without the connectivity preserving strategy. Fig. 2 shows the velocity errors between the spacecraft in formation. It can be observed that the steady-state errors of relative velocity are less than $10^{-3}m/s$. In Fig. 3, the maximum value of $||\boldsymbol{\rho}_{12}||$ and $||\boldsymbol{\rho}_{13}||$ are around $169.3m$ and $147.4m$, respectively. These distances are larger that the communication range so that spacecraft 1 lose communication with the other two spacecraft and the formation mission cannot be completed. The control forces (described in the body reference coordinate) are shown in Fig. 4.

In contrast, Figs. 5, 6 and 7 show the corresponding results of velocity errors, distance and control force with the connectivity preserving strategy. Fig. 6 shows the distances between the spacecraft in formation. It can be seen that after around $3000s$, the distances between any two spacecraft in formation are close to $60m$, meeting the requirements of forming specific configuration. In Fig. 6, the maximum distances between all spacecraft decrease to about $110m$, which is smaller than the communication range. So the communication graph is connected during all times of the formation missions. In addition, the distances between any two spacecraft in formation are larger than $10m$, there is no collisions between any spacecraft. Therefore, no collision occurs and no communication links will be lost during SFF. The control forces (described in the body reference coordinate) are shown in Fig. 7.

This comparison shows that the attraction potential function can ensure that the distance between any two spacecraft will smaller than Δ if they have communication links between each other. More specifically, the connectivity of the communication graph is preserved and then all spacecraft will converge to the given configuration through this connected graph.

5 Conclusions

In the paper, the effect of relative distance on communication graph and collision avoidances between spacecraft in SFF are investigated. The design philosophy is to construct an artificial potential function, which including the attraction part and repulsion part. The uncertainty of the mass of spacecraft is also considered. The proposed controller guarantees the connectivity of communication graph during SFF. Therefore, each spacecraft can transfer their states to all other spacecraft through the connected graph. This property is quite significant for distributed SFF. In future

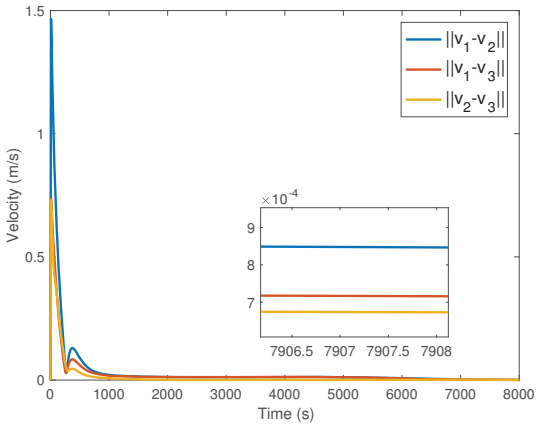

Fig. 2: Norm of velocity errors

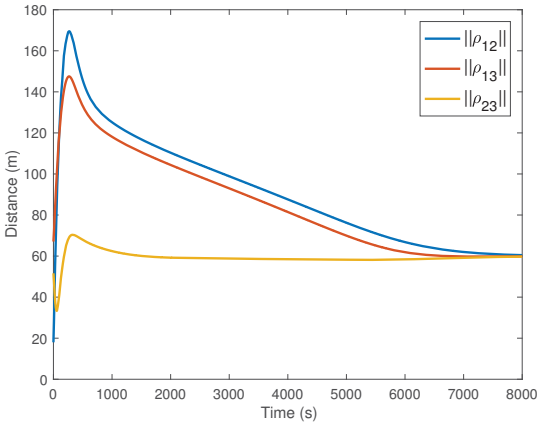

Fig. 3: Distance

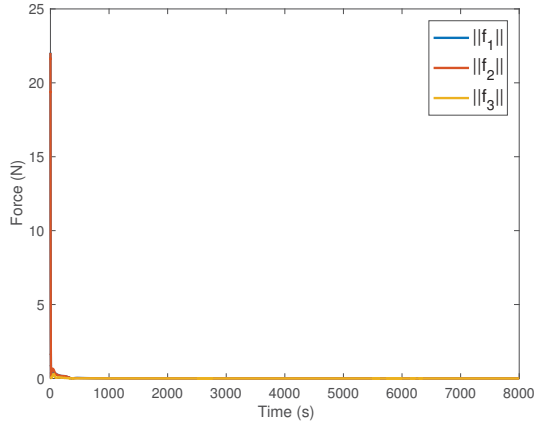

Fig. 4: Norm of control force

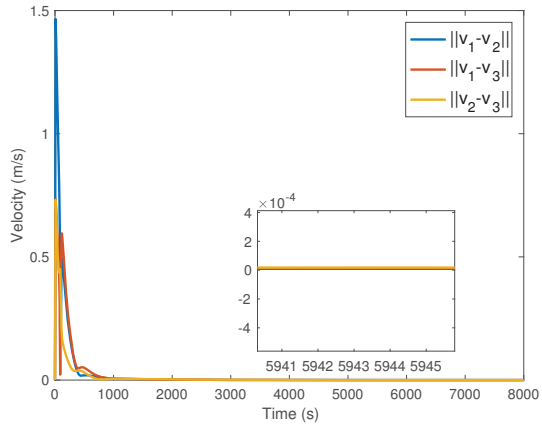

Fig. 5: Norm of velocity errors ($\Delta = 120m$).

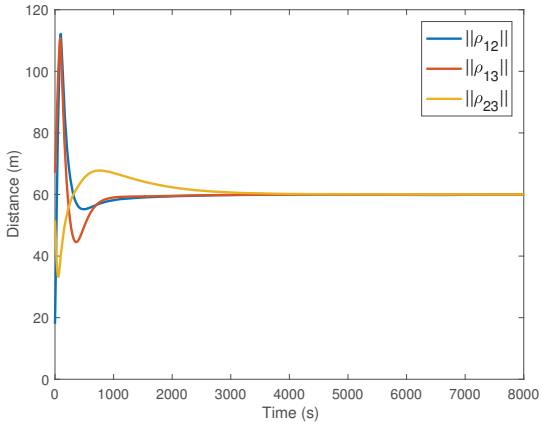

Fig. 6: Distance ($\Delta = 120m$).

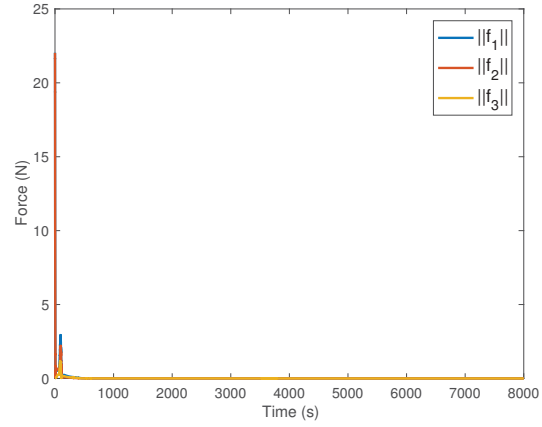

Fig. 7: Norm of control force ($\Delta = 120m$).

work, the extension of the presented control algorithm using non-certainty equivalence for formation problem can be planned. Another direction involves considering the connectivity maintenance of a directed graph for SFF.

References

[1] K. Alfriend, S. R. Vadali, P. Gurfil, J. How, and L. Breger, *Spacecraft formation flying: Dynamics, control and navigation*, vol. 2. Elsevier, 2009.

[2] R. Schlanbusch, R. Kristiansen, and P. J. Nicklasson, "Spacecraft formation reconfiguration with collision avoidance," *Automatica*, vol. 47, no. 7, pp. 1443–1449, 2011.

[3] G. Di Mauro, M. Lawn, and R. Bevilacqua, "Survey on guidance navigation and control requirements for spacecraft formation-flying missions," *Journal of Guidance, Control, and Dynamics*, vol. 41, no. 3, pp. 581–602, 2017.

[4] G. Liu and S. Zhang, "A survey on formation control of small satellites," *Proceedings of the IEEE*, vol. 106, no. 3, pp. 440–457, 2018.

[5] S. Bandyopadhyay, G. P. Subramanian, R. Foust, D. Morgan, S.-J. Chung, and F. Hadaegh, "A review of impending small satellite formation flying missions," in *53rd AIAA Aerospace Sciences Meeting*, p. 1623, 2015.

[6] D. P. Scharf, F. Y. Hadaegh, and S. R. Ploen, "A survey of spacecraft formation flying guidance and control. part ii: Control," *American Control Conference*, vol. 4, pp. 2976–2985, 2004.

[7] T. Balch and R. C. Arkin, "Behavior-based formation control for multirobot teams," *IEEE transactions on robotics and automation*, vol. 14, no. 6, pp. 926–939, 1998.

[8] M. Sabatini and G. B. Palmerini, "Collective control of spacecraft swarms for space exploration," *Celestial Mechanics and Dynamical Astronomy*, vol. 105, no. 1-3, p. 229, 2009.

[9] N. Zhou, R. Chen, Y. Xia, and J. Huang, "Finite-time formation reconfiguration of multiple spacecraft with collision avoidance problems," in *Proceedings of the 35th Chinese Control Conference*, pp. 3200–3205, 2016.

[10] Q. Hu, H. Dong, Y. Zhang, and G. Ma, "Tracking control of spacecraft formation flying with collision avoidance," *Aerospace Science and Technology*, vol. 42, pp. 353–364, 2015.

[11] D. Lee, A. K. Sanyal, and E. A. Butcher, "Asymptotic tracking control for spacecraft formation flying with decentralized collision avoidance," *Journal of Guidance, Control, and Dynamics*, vol. 38, no. 4, pp. 587–600, 2014.

[12] X. Huang, Y. Yan, Y. Zhou, and Y. Yang, "Dual-quaternion based distributed coordination control of six-dof spacecraft formation with collision avoidance," *Aerospace Science and Technology*, vol. 67, pp. 443–455, 2017.

[13] M. Ji and M. Egerstedt, "Distributed coordination control of multiagent systems while preserving connectedness," *IEEE Transactions on Robotics*, vol. 23, no. 4, pp. 693–703, 2007.

[14] H. Fang, Y. Wei, J. Chen, and B. Xin, "Flocking of second-order multiagent systems with connectivity preservation based on algebraic connectivity estimation," *IEEE transactions on cybernetics*, vol. 47, no. 4, pp. 1067–1077, 2017.

[15] R. Kristiansen and P. J. Nicklasson, "Spacecraft formation flying: a review and new results on state feedback control," *Acta Astronautica*, vol. 65, no. 11-12, pp. 1537–1552, 2009.

[16] M. Mesbahi and M. Egerstedt, *Graph theoretic methods in multiagent networks*, vol. 33. Princeton University Press, 2010.